Published by Institute of Physics Publishing for SISSA
Received: *May 25, 2008*
Accepted: *July 1, 2008*
Published: *July 15, 2008*

Reconciling results of LSND, MiniBooNE and other experiments with soft decoherence

Yasaman Farzan
Institute for research in fundamental sciences (IPM),
PO Box 19395-5531, Tehran, Iran
E-mail: yasaman@theory.ipm.ac.ir

Thomas Schwetz
Theory Division, Physics Department, CERN, 1211 Geneva 23, Switzerland
E-mail: schwetz@cern.ch

Alexei Yu Smirnov
International Centre for Theoretical Physics,
Strada Costiera 11, 34014 Trieste, Italy, and
Institute for Nuclear Research, Russian Academy of Sciences, Moscow, Russia
E-mail: smirnov@ictp.it

Abstract: We propose an explanation of the LSND signal via quantum-decoherence of the mass states, which leads to damping of the interference terms in the oscillation probabilities. It is assumed that decoherence mainly affects the state ν_3 (oscillations with the atmospheric Δm^2) and damping effects rapidly decrease with the neutrino energy (the decoherence parameter $\gamma \propto E_\nu^{-4}$). This allows us to reconcile the positive LSND signal with MiniBooNE and other null-result experiments. The standard explanations of solar, atmospheric, KamLAND and MINOS data are not affected. No new particles, and in particular, no sterile neutrinos are needed. The model does not explain the low-energy MiniBooNE anomaly and does not resolve the LSND-KARMEN tension. The LSND signal is controlled by the 1-3 mixing angle θ_{13} and, depending on the degree of damping, yields $0.0014 < \sin^2\theta_{13} < 0.034$ at 3σ. The scenario can be tested at upcoming θ_{13} searches: while the comparison of near and far detector measurements at reactors should lead to a null-result a positive signal for θ_{13} is expected in long-baseline accelerator experiments. The proposed decoherence may partially explain the results of Gallium detector calibrations and it can strongly affect supernova neutrino signals.

Keywords: Neutrino Physics, Beyond Standard Model.

JHEP07(2008)067

Contents

JHEP07(2008)067

1. Introduction

Reconciling the LSND signal for $\bar{\nu}_\mu \to \bar{\nu}_e$ transitions [1] with the by now fully established existence of neutrino oscillations [2 – 6] on the one hand side and bounds on oscillations [7 – 13] on the other is a long-standing problem in neutrino physics. Recently the MiniBooNE experiment [14] failed to confirm the oscillation interpretation of the LSND signal [15], putting further pressure on its interpretation. Usually the LSND result is considered as an indication for sterile neutrino oscillations, despite difficulties of the corresponding models to explain the global data [16] including cosmological observations (see ref. [17] for a recent analysis including the MiniBooNE results). Triggered by these problems many ideas and scenarios have been proposed in order to explain LSND, some of them involving very exotic physics. This includes sterile neutrino decay [18, 19], violation of the CPT [20] and/or Lorentz [21] symmetries, mass-varying neutrinos [22], short-cuts of sterile neutrinos in extra dimensions [23], a non-standard energy dependence of the sterile neutrino parameters [24], or sterile neutrinos interacting with a new gauge boson [25].

In the present paper, we revisit the possibility that the origin of the LSND signal might be quantum decoherence in neutrino oscillations [26, 27]. Such effects can be induced by interactions with a stochastic environment; a possible source for this kind of effect might be quantum gravity [28 – 30], see ref. [31] for a recent discussion. We take a phenomenological approach and determine the form and magnitude of the new effects from observations without reference to possible origins of the decoherence. Neutrino oscillations, being a quantum interference effect over macroscopic distances, provide a sensitive

test for decoherence. The possibility to use neutrinos as a probe of quantum decoherence has been explored for atmospheric neutrinos [32], solar neutrinos [33], KamLAND [33, 34], future long-baseline experiments [35, 36], and neutrino telescopes [37]. See also ref. [38]. Other quantum systems which have been considered to search for decoherence include, for example, $K\bar{K}$ [29, 39, 40] and $B\bar{B}$ [41, 42] oscillations or neutron interferometry [43]. Throughout this paper we will assume that quantum decoherence affects only the neutrino sector.

Previous attempts to explain the LSND signal by quantum decoherence [26, 27] seem to be in conflict with the present data. Indeed, for the set-up of NuTeV with a baseline of ~ 1 km and the average energy of 75 GeV the model in [27] predicts $P(\nu_\mu \to \nu_e) = P(\bar{\nu}_\mu \to \bar{\nu}_e) = 3 \times 10^{-3}$ while the one in [26] yields $P(\bar{\nu}_\mu \to \bar{\nu}_e) = 0.2$. Both of these predictions strongly violate the upper bound on the neutrino and anti-neutrino oscillation probabilities from NuTeV: $P(\nu_\mu \to \nu_e), P(\bar{\nu}_\mu \to \bar{\nu}_e) < 5 \times 10^{-4}$ (90% C.L.) [13]. Furthermore, the model of [26] (where in addition to decoherence, also CPT-violation is also introduced) cannot account for the spectral distortion in the anti-neutrino signal observed by KamLAND. The scenario of [27] is also disfavored by the absence of a signal in KARMEN [9], NOMAD [12] and MiniBooNE [14]. In the present paper we propose a different set of decoherence parameters with a special energy dependence. As a result, the problems outlined above can be avoided. In our scenario, the decoherence effects become more significant with decreasing the energy; thus, we refer to this scenario as "*soft decoherence*".

The paper is organized as follows. In section 2, we describe our scenario of the decoherence effect and discuss how the LSND signal is explained. In section 3, we show that by selecting suitable parameters, within this scenario the LSND result can be reconciled with all other oscillation results (both positive and negative). In section 4, we discuss how this scenario can be checked in forthcoming and future experiments. Discussions and conclusions will be presented in section 5.

2. The scenario: decoherence and the LSND result

2.1 Soft decoherence

Let us describe the neutrino system by the density matrix ρ in the mass state basis, ν_i, $i = 1, 2, 3$. The decoherence effects in the evolution of the density matrix can be parameterized by introducing a new term $\mathcal{D}[\rho]$ as

$$\frac{d\rho}{dt} = -i[H, \rho] - \mathcal{D}[\rho]\,. \tag{2.1}$$

This term violates the conservation of $\mathrm{Tr}(\rho^2)$ and, hence, leads to the evolution of pure states into mixed states. As mentioned in introduction, such a term can be induced by interaction with a stochastic environment; a possible source for this kind of effect might be quantum gravity [28 – 30]. The form of the operator $\mathcal{D}[\rho]$ can be constrained by imposing some general requirements on the evolution of the system. First, *complete positivity* implies the so-called Lindblad form for $\mathcal{D}[\rho]$ [44, 45]:

$$\mathcal{D}[\rho] = \sum_n \left[\{\rho, D_n D_n^\dagger\} - 2 D_n \rho D_n^\dagger\right]\,. \tag{2.2}$$

JHEP07(2008)067

where D_n are some general complex matrices. This form arises from "tracing away" the dynamics of the environment [30, 46]. Second, with general complex D_n unitarity is violated, i.e., $d\mathrm{Tr}(\rho)/dt$ can be nonzero. Therefore, we require that D_n are Hermitian, $D_n^\dagger = D_n$. In addition to $d\mathrm{Tr}(\rho)/dt = 0$, the Hermiticity of D_n guarantees that the entropy [i.e., $S(\rho) = -\mathrm{Tr}(\rho \ln \rho)$] cannot decrease [45, 47]. Finally, we require that the average energy of the system, $\mathrm{Tr}(\rho H)$, is conserved. It is straightforward to check that this can be achieved by demanding $[H, D_n] = 0$. In other words, unitarity and conservation of the energy-momentum imply that D_n and H can be simultaneously diagonalized. In the neutrino mass basis, we can therefore write

$$H = \mathrm{Diag}[h_1, h_2, h_3] \quad \text{and} \quad D_n = \mathrm{Diag}[d_{n,1}, d_{n,2}, d_{n,3}]\,, \tag{2.3}$$

where $h_i^2 \equiv p^2 + m_i^2$, and $d_{n,i}$ are real quantities of dimension $[\mathrm{mass}]^{1/2}$ whose energy-dependence is unknown. In this paper we adopt a phenomenological approach and determine $d_{n,i}$ from observations without discussing their possible origins.

Solving the evolution equation eq. (2.1), with H and D_n given in (2.3) we find

$$\rho(t) = \begin{bmatrix} \rho_{11}(0) & \rho_{12}(0)e^{-(\gamma_{12}-i\Delta_{12})t} & \rho_{13}(0)e^{-(\gamma_{13}-i\Delta_{13})t} \\ \rho_{21}(0)e^{-(\gamma_{21}-i\Delta_{21})t} & \rho_{22}(0) & \rho_{23}(0)e^{-(\gamma_{23}-i\Delta_{23})t} \\ \rho_{31}(0)e^{-(\gamma_{31}-i\Delta_{31})t} & \rho_{32}(0)e^{-(\gamma_{32}-i\Delta_{32})t} & \rho_{33}(0) \end{bmatrix}, \tag{2.4}$$

where $\rho_{ij}(0)$ are the elements of the density matrix at the initial moment,

$$\gamma_{ij} \equiv \sum_n (d_{n,i} - d_{n,j})^2 \quad \text{and} \quad \Delta_{ji} \equiv h_j - h_i \approx \frac{\Delta m^2_{ji}}{2E_\nu}\,. \tag{2.5}$$

Notice that $\gamma_{ij} = \gamma_{ji}$ whereas $\Delta_{ij} = -\Delta_{ji}$, and the diagonal elements of ρ do not depend on time.

Let us consider the transitions between the flavor states, $\nu_\alpha = \sum_i U_{\alpha i}\nu_i$, where $U_{\alpha i}$ are the elements of the PMNS mixing matrix. The probability of finding a neutrino with flavor β is given by $\langle \nu_\beta | \rho | \nu_\beta \rangle$. Hence, the oscillation probability $\nu_\alpha \to \nu_\beta$ in vacuum is equal to

$$P_{\alpha\beta} = \langle \nu_\beta | \rho^{(\alpha)}(t) | \nu_\beta \rangle = \sum_{ij} U^*_{\beta i} U_{\beta j}\, \rho^{(\alpha)}_{ij}(t)\,, \tag{2.6}$$

where $\rho^{(\alpha)}_{ij}(t)$ is given by eq. (2.4) with $\rho_{ij}(0) = \rho^{(\alpha)}_{ij}(0) = U_{\alpha i}U^*_{\alpha j}$, which corresponds to the initial state ν_α.

In this paper, we consider the most economic scenario that describes all the data. As we will show in the following, only one matrix D_n with

$$d_1 = d_2 \neq d_3 \tag{2.7}$$

is sufficient. Note that a similar pattern exists between neutrino masses ($m_1 \simeq m_2 \neq m_3$), so it will be inspiring to build a model that links the patterns of H and D. eq. (2.7) leads to

$$\gamma_{12} = 0 \quad \text{and} \quad \gamma \equiv \gamma_{13} = \gamma_{32}\,. \tag{2.8}$$

In the ranges of energy and baseline (L) for which $\Delta_{21}L = \Delta m^2_{21}L/(2E_\nu) \ll 1$, the oscillations due to Δm^2_{21} can be neglected, and eq. (2.6) yields

$$\begin{aligned} P_{\mu e}(\gamma, L) &= P_{e\mu}(\gamma, L) = 2|U_{\mu 3}|^2|U_{e3}|^2 \left[1 - e^{-\gamma L}\cos(\Delta_{31}L)\right] , \\ P_{ee}(\gamma, L) &= 1 - 2|U_{e3}|^2(1 - |U_{e3}|^2) \left[1 - e^{-\gamma L}\cos(\Delta_{31}L)\right] , \\ P_{\mu\mu}(\gamma, L) &= 1 - 2|U_{\mu 3}|^2(1 - |U_{\mu 3}|^2) \left[1 - e^{-\gamma L}\cos(\Delta_{31}L)\right] . \end{aligned} \tag{2.9}$$

Notice that although the new term $\mathcal{D}[\rho]$ explicitly breaks the time reversal symmetry, still within the framework of the two-neutrino oscillation the equality $P_{e\mu} = P_{\mu e}$ holds. In principle, the decoherence effects can give rise to the CPT violation; however, in this paper we assume that the decoherence effects in the neutrino and antineutrino sectors are the same.

The energy dependence of the decoherence parameter γ in eq. (2.8) is not known; it should follow from a microscopic theory of decoherence. In the absence of such a theory we assume a power law: $\gamma \propto E_\nu^{-r}$, and for convenience parameterize it as

$$\gamma = \frac{\mu^2}{E_\nu}\left(\frac{40\ \text{MeV}}{E_\nu}\right)^{r-1} , \tag{2.10}$$

where 40 MeV is the typical neutrino energy in LSND. We will estimate the allowed ranges of parameters r and μ^2 in section 3, and in particular, show that all the data can be described if

$$r = 4 , \tag{2.11}$$

which we will use as the reference value in our estimations. The fast decrease of γ, and consequently, the decoherence effect with energy, is the key feature of the proposed scenario which allows us to reconcile the LSND result with results of other experiments. Notice that for any value of $r \neq 1$, the Lorentz symmetry is explicitly violated.

2.2 Explaining LSND events

Let us now discuss the interpretation of the positive LSND result through soft decoherence. For the LSND parameters, $E \sim 40\,\text{MeV}$ and $L \simeq 30$ m, the oscillation phase $\Delta_{31}L \sim 5 \cdot 10^{-3}$, so that the oscillation effect is negligible and according to (2.9) the appearance probability is equal to

$$P_{\mu e}(\gamma, L) = 2|U_{\mu 3}|^2|U_{e3}|^2 \left(1 - e^{-\gamma L}\right) \approx |U_{e3}|^2 \left(1 - e^{-\gamma L}\right) . \tag{2.12}$$

Hence, the LSND signal is determined by the 1-3 mixing and the degree of decoherence given by the factor $(1 - e^{-\gamma L})$. In the case of strong decoherence, $\gamma L \gg 1$, this factor converges to its maximum and

$$P_{\mu e}(\gamma, L) \approx |U_{e3}|^2 . \tag{2.13}$$

The LSND signal is simply given by the 1-3 mixing parameter, and therefore the LSND probability provides a lower bound on the 1-3 mixing:

$$|U_{e3}|^2 \geq P_{\mu e}^{\text{LSND}} = (2.6 \pm 0.8) \cdot 10^{-3} . \tag{2.14}$$

JHEP07(2008)067

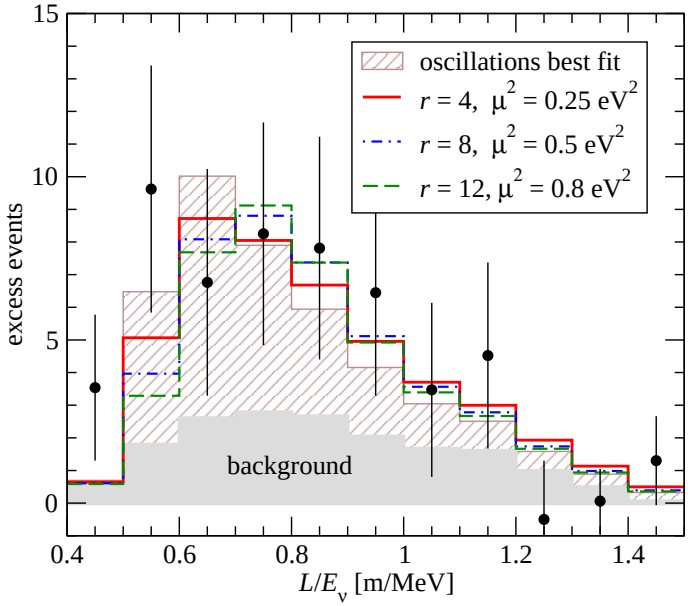

Figure 1: Spectrum of $\bar{\nu}_e$ excess events in LSND. The histograms correspond to the prediction of the decoherence scenario for various values of r, see eq. (2.10). The best fit value for μ^2 in each case is assumed.

For a small decoherence effect, $\gamma L \ll 1$, we obtain

$$P_{\mu e}(\gamma, L) \approx |U_{e3}|^2 \, \gamma L \, . \tag{2.15}$$

Therefore $|U_{e3}|^2$ can be as large as the upper bound obtained from the reactor experiments and other observations, $(|U_{e3}|^2)^{\rm upper}$. In this case the LSND result gives a lower bound on γ at typical LSND energies:

$$\gamma \geq \frac{P_{\mu e}^{\rm LSND}}{(|U_{e3}|^2)^{\rm upper} L_{\rm LSND}} \, . \tag{2.16}$$

In figure 1 we show the L/E dependence of the excess of the LSND events. The points with error bars are the LSND data and the histograms show the prediction of the decoherence scenario (added to the background) for various values of the power r, see eq. (2.10). To draw each histogram, the corresponding best fit value for μ^2 is assumed. For comparison we show the spectrum expected due to oscillations in the model with a light sterile neutrino. The decoherence reproduces the observed spectrum quite well. It leads to a softer energy spectrum than the oscillation spectrum. Furthermore, with increase of r the softness increases and the maximum shifts to lower energies. Unfortunately these differences are small and with the LSND statistics and uncertainties it is not possible to distinguish decoherence and oscillation effects or substantially restrict r for $r \geq 4$. For $\gamma L \sim 1$, $L \simeq 30$ m and typical LSND neutrino energies $E_\nu \sim 40\,\text{MeV}$, the relevant scale for the parameter μ introduced in eq. (2.10) is $\mu^2 \sim 0.1$ eV^2.

Thus, in the proposed scenario the LSND $\bar{\nu}_\mu \to \bar{\nu}_e$ signal is explained by the decoherence of the mass state ν_3, whose mixing with ν_μ and ν_e are given by $\cos\theta_{13} \sin\theta_{23}$ and

JHEP07(2008)067

$\sin\theta_{13}$, respectively. The oscillation effect is negligible and plays no role here. Linking the LSND signal with the last unknown mixing angle, θ_{13}, is an exciting feature of the model. We will discuss the implications of this relation in section 4.

3. Reconciling LSND with other observations

To simultaneously accommodate the positive LSND signal and the lack of any evidence for flavor transitions from other short-baseline experiments, the value and energy-dependence of γ have to be properly chosen. In what follows, we demonstrate that since the neutrino energy and baseline for each experiment are different, such a choice is possible without affecting the successful description of solar, atmospheric, KamLAND, and MINOS data in terms of neutrino oscillations.

3.1 Short baseline and reactor experiments

In short-baseline experiments, $\Delta m^2_{ij} L/(2E_\nu) \ll 1$ and we can neglect oscillations. Therefore, for a given power r there are three parameters to describe these experiments: μ^2, $|U_{e3}|^2 \equiv \sin^2\theta_{13}$ and $|U_{\mu 3}|^2 \equiv \cos^2\theta_{13}\sin^2\theta_{23}$ [see eq. (2.9)]. Hence, this scenario involves the same number of parameters as the (3+1) sterile neutrino oscillation schemes. We have performed a fit to the data from LSND [1] (decay-at-rest data), KARMEN [9], MiniBooNE [14, 48], NOMAD [12], CDHS [10], and the reactor experiments Bugey [11], Chooz [7], and Palo Verde [8]. For technical details, see refs. [17, 49]. Results of the fit are shown in the μ^2-$|U_{e3}|^2$ plane in figure 2.

The LSND signal can be reconciled with the null-result from KARMEN (which has the same neutrino energy as LSND) due to the somewhat shorter baseline in KARMEN ($L \simeq 18$ m) and the exponential dependence of the decoherence effect on the distance. The solid and dashed curves in figure 2 show the allowed regions from LSND and KARMEN, respectively. At 99% C.L., there is a significant overlap left, though there remains some tension between the two results. Notice that a similar tension exists in other scenarios developed to explain the LSND results such as the case of oscillations [15, 50] or sterile neutrino decay [19], the latter having the same exponential L dependence as in the decoherence model.

The baseline and energy of neutrinos at MiniBooNE are one order of magnitude larger than in LSND. As a result, the oscillation phase $\Delta m^2 L/(2E_\nu)$ for the two experiments are of the same order and oscillations can be neglected. We find that for $r > 2$, at MiniBooNE $\gamma L \ll 1$ and therefore the decoherence effects are negligible, rendering the new effects at MiniBooNE unobservable and explaining the non-observation of an appearance signal. As visible in figure 2, for MiniBooNE the decoherence becomes important only for $\mu^2 \gtrsim 20\,\mathrm{eV}^2$, and is completely negligible for values of μ relevant for LSND. Similarly to the case of standard oscillations, the soft decoherence cannot account for the event excess observed in MiniBooNE below 475 MeV. Therefore, following ref. [14], we rely on a yet to be identified explanation of this excess and use only the data above 475 MeV in the analysis.

At the reference value $r = 4$ any decoherence effect for short baseline experiments with energies substantially larger than 40 MeV is suppressed. This implies no flavor tran-

JHEP07(2008)067

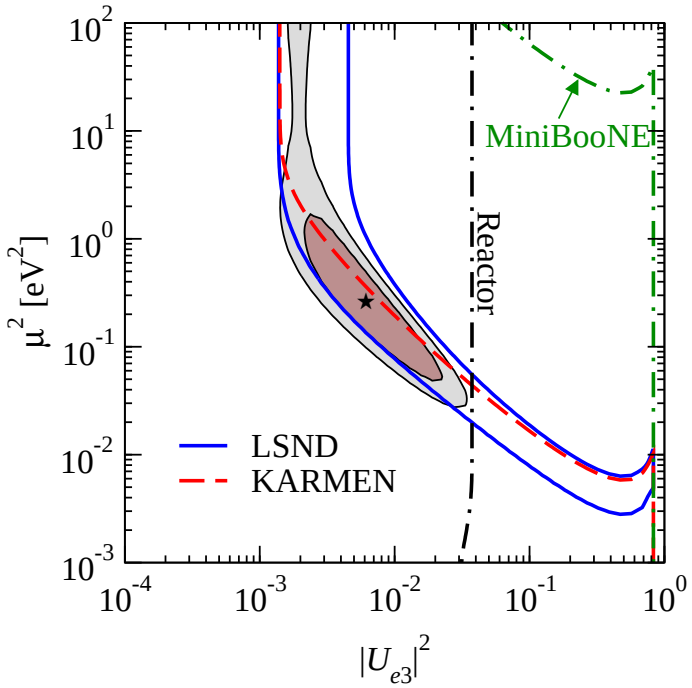

Figure 2: Allowed regions in the plane of $|U_{e3}|^2$ and the decoherence parameter μ^2 for $r = 4$. Shaded regions: global data at 90% and 99% CL. Curves: 99% CL regions from LSND, KARMEN, MiniBooNE and reactor data (Bugey, Chooz, Palo Verde). The star marks the global best fit point. We marginalize over $\sin^2\theta_{23}$ taking into account the constraint from atmospheric neutrinos.

sitions in the "high energy" experiments ($E_\nu \gtrsim 0.5\,\text{GeV}$) MiniBooNE, NOMAD, NuTeV, and CDHS.[1] Therefore, our scenario is trivially consistent with the null-result of these experiments.

The energies of reactor neutrinos are relatively low (of order 4 MeV). As a result, for these neutrinos γ is quite large:

$$\gamma \sim 2.5\,\frac{\mu^2}{0.2\text{ eV}^2}\left(\frac{4\text{ MeV}}{E_\nu}\right)^4\text{ cm}^{-1}\,. \tag{3.1}$$

Thus, already after a few centimeters coherence is completely lost and the survival probability in eq. (2.9) becomes independent of the energy and baseline:

$$P_{\bar{e}\bar{e}}^{\text{reactor}} \simeq 1 - 2|U_{e3}|^2(1-|U_{e3}|^2)\,. \tag{3.2}$$

Thus, the Chooz bound on $P_{\bar{e}\bar{e}}$, which is derived by comparing the measured $\bar{\nu}_e$ flux at a distance of 1 km from the source with the estimated flux from the consideration of the power of the reactor can be directly translated into an upper bound on $|U_{e3}|^2$. The upper bound on $|U_{e3}|^2$ from the combination of Chooz, Bugey and Palo Verde data is shown in figure 2. We find $|U_{e3}|^2 < 0.04$ at 3σ (1 d.o.f.).

[1] A similar strategy to reconcile low and high energy short-baseline data has been pointed out in ref. [24] in the context of sterile neutrinos with a non-standard energy dependence.

JHEP07(2008)067

	(3+2) oscillations		decoherence	
Data sets	$\chi^2_{\rm PG}$/d.o.f.	PG	$\chi^2_{\rm PG}$/d.o.f.	PG
LSND vs NEV	21.2/5	0.08%	8.6/2	1.4%
App vs Disapp	17.2/4	0.18%	0.6/2	74%

Table 1: Consistency of LSND versus all other no-evidence short-baseline data (NEV), and appearance versus disappearance short-baseline data for (3+2) oscillations and the decoherence model. We give $\chi^2_{\rm PG}$ according to eq. (3.5) and the corresponding probability ("PG"). The results for (3+2) are taken from table 3 of ref. [17].

The shaded regions in figure 2 show the results of the global analysis of the short-baseline experiments. We include $\sin^2\theta_{23}$ as a free parameter in the fit, taking into account the standard constraint from the Super-Kamiokande atmospheric neutrino data [2], which is hardly affected by decoherence (see next section for a more detailed discussion). For $r = 4$ we find the best fit point at

$$|U_{e3}|^2 = 6.1 \times 10^{-3}\,, \qquad \sin^2\theta_{23} = 0.5\,, \qquad \mu^2 = 0.27\,\mathrm{eV}^2\,, \tag{3.3}$$

with $\chi^2_{\rm min} = 89/(107-3)$ d.o.f. For these values of the parameters, the averaged probability in LSND equals $P^{\rm LSND}_{\mu e} = 2.3 \cdot 10^{-3}$ which is within one sigma of the experimental value $(2.6 \pm 0.8) \cdot 10^{-3}$. The allowed range for $|U_{e3}|^2$ is

$$(1.4)\, 2.3 \times 10^{-3} < |U_{e3}|^2 < 2.1\,(3.4) \times 10^{-2} \qquad \text{at } 2\ (3)\sigma\ (1\text{ d.o.f.})\,. \tag{3.4}$$

Here the lower bound follows from the LSND result in the limit of strong decoherence, see eq. (2.14). The upper bound comes from the reactor experiments.

Let us evaluate the quality of the fit in more detail, and compare it to the case of sterile neutrino oscillations in a (3+2) scheme [51]. To this aim we divide the data into sub-sets and check the consistency of these data sets by using the so-called Parameter Goodness-of-fit (PG) criterion [16, 52]. It is based on the χ^2 function

$$\chi^2_{\rm PG} = \chi^2_{\rm tot,min} - \sum_i \chi^2_{i,\rm min}\,, \tag{3.5}$$

where $\chi^2_{\rm tot,min}$ is the χ^2 minimum of all data sets combined and $\chi^2_{i,\rm min}$ is the minimum of the data set i. This χ^2 function measures the "price" one has to pay by the combination of the data sets compared to fitting them independently. It should be evaluated for the number of d.o.f. corresponding to the number of parameters in common to the data sets, see ref. [52] for a precise definition.

First we test the consistency of LSND with all the other null-result short-baseline experiments (NEV). The numbers given in table 1 show that for (3+2) oscillations LSND is consistent with NEV only with a probability of 0.08%, whereas in the decoherence scenario the probability improves to 1.4%. Note that in the (3+2) case short-baseline data depend on 7 parameters, whereas for decoherence only 3 parameters are available to fit the data.[2]

[2]As before we work at fixed $r = 4$ and do not consider the energy exponent as a free parameter.

JHEP07(2008)067

The reason for the still relatively low probability of 1.4% is the aforementioned tension between the LSND and KARMEN results. In order to illustrate this effect we perform a second test, dividing the data into appearance experiments (LSND, KARMEN, NOMAD, MiniBooNE) and disappearance experiments (CDHS, Bugey, Chooz, Palo Verde). In this approach, LSND and KARMEN data are summed into the same data set and therefore, by assumption they are taken to be consistent. As a result, the remaining tension between them does not show up in the PG test. Note that it is reasonable to combine LSND and MiniBooNE into the same data set, because in both cases considered here they are consistent: for (3+2) oscillations they can be reconciled [17] by invoking CP violation [19, 53], whereas in the decoherence scenario the energy dependence of γ guarantees the null-result of MiniBooNE. As shown in table 1, we find an excellent fit in the decoherence model (PG of 74%), whereas (3+2) oscillations suffer from a sever tension between appearance and disappearance experiments, allowing for compatibility with a probability of only 0.18%.

In summary, the soft decoherence proposed here provides an excellent fit to short-baseline experiments, allowing for full consistency of LSND and MiniBooNE, as well as appearance and disappearance experiments. Only the well-known tension between LSND and KARMEN remains unresolved.

3.2 Other phenomenological consequences

In this section, we show that our scenario is compatible with the standard description of the solar [5], KamLAND [6], atmospheric [2], K2K [4] and MINOS [3] data in terms of neutrino oscillations.

Solar and long-baseline reactor neutrino data: in ref. [33], decoherence effects on solar and KamLAND neutrino data have been studied (see also ref. [34] for the case of KamLAND only). The decoherence scenario in [33] differs from the one in the present paper: While we take $\gamma_{12} = 0$ ($d_1 = d_2$) and discuss the effects of $\gamma = (d_1 - d_3)^2$, the authors of [33] focused on the effects of $\gamma_{12} \equiv (d_1 - d_2)^2$. Our assumption $d_1 = d_2$ in eq. (2.7) ensures that oscillations in the 1-2 sector are not affected by decoherence. This leaves the dominant oscillations due to Δm^2_{21} and θ_{12} unchanged and guarantees the standard oscillation explanations for the solar and KamLAND data. Within our scenario, the effects of the damping factor on the solar neutrino flux and KamLAND neutrinos are suppressed by $|U_{e3}|^2$. The current uncertainties do not allow to resolve the effects of $|U_{e3}|^2$. Moreover, in these experiments oscillations due to Δm^2_{31} are completely averaged out and therefore decoherence effects in the 1-3 sector are unobservable.

We can use results of [33] to put an upper bound on $\gamma_{12} = (d_1 - d_2)^2$. Writing $\gamma_{12} \equiv \gamma_0 (1\,\mathrm{GeV}/E_\nu)^r$, in ref. [33] bounds on γ_0 have been derived from solar and KamLAND data assuming $r = 0, \pm 1, \pm 2$. Extrapolating these results to $r = 4$, one finds $\gamma_0 < 10^{-32}\,\mathrm{GeV}$. Using the parametrization shown in eq. (2.10), one has $\gamma_0 = 6.4 \cdot 10^{-23}\,\mathrm{GeV}\,(\mu^2_{12}/\mathrm{eV}^2)$, and

$$\mu^2_{12} < 10^{-10}\ \mathrm{eV}^2 \ll \mu^2\,. \tag{3.6}$$

Atmospheric neutrinos: first, we note that because of the smallness of $|U_{e3}|^2$, the decoherence effects do not considerably change the ν_e flux at low energies where the Earth

JHEP07(2008)067

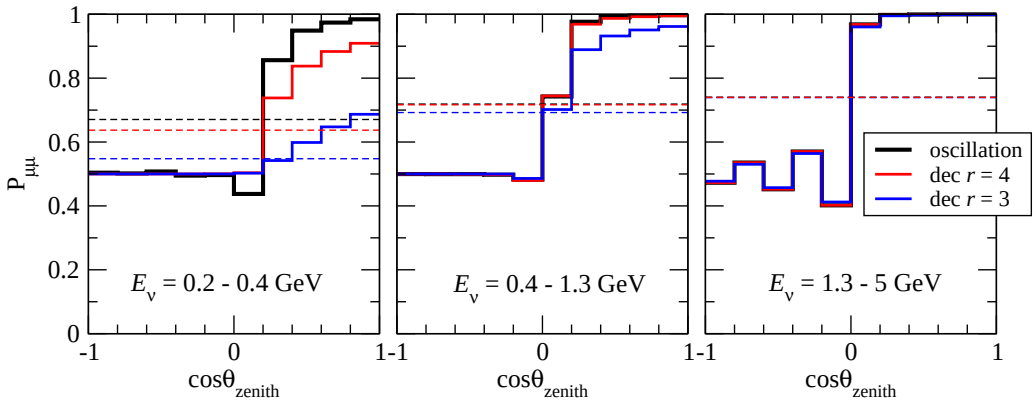

Figure 3: The zenith angle dependence of the ν_μ survival probability relevant for atmospheric neutrinos in three different energy intervals for $r = 3, 4$ and for the case of oscillations without decoherence. The horizontal dashed lines show the corresponding probabilities averaged over all zenith angles.

matter effect can be neglected. For high energies (multi-GeV sample) where the 1-3 mixing is enhanced the decoherence effect becomes negligible. However, the muon neutrino disappearance probability can be significantly affected. In order to have a detectable effect of decoherence, the neutrino energies and baselines should be in a range for which $\gamma L \gtrsim 1$ and $\Delta_{31} L \lesssim 2\pi$. For $\Delta_{31} L \gg 2\pi$, regardless of the value of γ, the interference term $e^{-\gamma L} \cos(\Delta_{31} L)$ averages out and the sensitivity to the new effects is lost. Putting the two conditions together, we find that the effects can be noticeable only for $E_\nu < 400\,\mathrm{MeV}$. On the other hand, for $E_\nu < 200\,\mathrm{MeV}$, the produced muons cannot be detected in Super-Kamiokande.

In figure 3 we show dependence of the survival probability $\nu_\mu \to \nu_\mu$ on the neutrino zenith angle for different energy ranges. In the lowest energy range, 200 MeV $< E_\nu <$ 400 MeV, the oscillation length $L_{\mathrm{osc}} = 2\pi E_\nu / \Delta m^2_{31} \sim 100$ km. Hence, the condition $\Delta_{31} L \sim \pi$ implies that only for neutrinos arriving from above (for zenith angles smaller than 90°) the damping effects are significant. As follows from figure 3, in the vertical direction for $r = 4$ and $r = 3$ the effect can reach 10% and 30%, correspondingly. However, for these low energies the direction of the initial neutrino is not related to the muon direction and hence, the distribution of μ-like events is averaged over the zenith angle. As a result, the decoherence leads to a zenith angle independent decrease of the sub-GeV μ-like events. The size of the effect is illustrated by the horizontal dashed lines in figure 3, which correspond to the zenith angle averaged survival probability. For 200 MeV $< E_\nu <$ 400 MeV, we find a suppression of 5% (18%) for $r = 4$ ($r = 3$). This effect can be detected as a decrease of the ratio of the μ-like to e-like events. We find that for $r \geq 4$ this decrease is below the 5% experimental uncertainty on this ratio [2]. Essentially this effect determines the lower bound on r. Let us note that at these low energies, there is some excess of e-like events in Super-K, which can be interpreted as renormalization and deficit of μ-like events and the latter can be explained by the decoherence in our scenario.

JHEP07(2008)067

In the energy interval 400 MeV $< E_\nu <$ 1.3 GeV the event suppression due to the decoherence effect is below 5% even for $r = 3$. The decoherence leads to a flattening of the zenith angle dependence. However, the averaging over the zenith angle in the μ-like events — though incomplete — is still strong. So uncertainties in the extraction of the zenith angle in the Super-Kamiokande experiment do not allow us to identify the effect of decoherence for $r > 3$. In the multi-GeV range the decoherence effect is strongly suppressed. In the Soudan experiment [54], in addition to the energy of the produced muon, the recoil energy of proton (in quasi-elastic interaction) is also measured. As a result, the zenith angle of the incoming neutrino can be deduced. However, in this experiment, the statistical error is larger than 10% and the decoherence effects cannot be resolved. We conclude that for $r \geq 4$ our scenario is consistent with the oscillation interpretation of atmospheric neutrino data.[3]

Long-baseline accelerator experiments: at MINOS [3] experiment with $E_\nu \gtrsim 2\,\text{GeV}$ and $L = 730$ km, the damping effect is very small, $(1 - e^{-\gamma L}) \approx \gamma L < 0.03$, and the present uncertainties do not allow to resolve the effect. In the K2K experiment [4] the energies of the neutrinos are smaller and the decoherence factor is slightly larger. However, still the statistics below GeV is too low for the experiment to be sensitive to the soft decoherence.

In ref. [32], the decoherence effects in the atmospheric and K2K neutrino data have been studied. However, the bounds derived in [32] do not apply here because we assume a steeper decrease of γ with energy.

Radioactive source experiments: in calibrations of the Gallium solar neutrino detectors SAGE [55] and GALLEX/GNO [56] with artificial radioactive ^{51}Cr and ^{37}Ar sources deficits of the signals have been reported in ref. [55]: the weighted average of the ratio of the observed to expected event numbers equals $R_{\text{Ga}} = 0.88 \pm 0.05$ [55]. This result was interpreted as an indication of electron neutrino disappearance due to oscillations into sterile neutrinos [57]. For the energies of the radioactive sources employed in these experiments, $E_\nu \sim 0.8\,\text{MeV}$, the damping parameter γ is huge [see eq. (3.1)] and the decoherence length $\sim 1/\gamma \sim 5 \cdot 10^{-4}$ cm. So, complete decoherence occurs over a small fraction of a millimeter and the survival probability is given by eq. (3.2). For the best fit value of $|U_{e3}|^2$ shown in eq. (3.3), we find a small effect: $P_{ee} \simeq 0.99$. However, if $|U_{e3}|^2$ is at its 3σ upper bound given in eq. (3.4) we obtain $P_{ee} \simeq 0.93$. The latter is within the 1σ range of R_{Ga} and therefore the results of the calibration experiments can be at least partially explained.

4. Future tests of the scenario

4.1 Reactors versus accelerators

The possibility to test decoherence effects at future long-baseline experiments has been discussed in [35, 36]. In our scenario, an explanation of the LSND signal implies a lower bound on the mixing angle θ_{13}. Therefore, upcoming oscillation experiments aiming at the measurement of this mixing angle will provide a crucial test.

[3] We thank Michele Maltoni for communication on this point.

JHEP07(2008)067

The next generation of reactor experiments like Double-Chooz [58], Daya Bay [59] and Reno [60] will search for θ_{13} by comparing the anti-neutrino flux measured at a near and far detector. As discussed in section 3.1, a remarkable consequence of our decoherence scenario is that for baselines larger than a few centimeters the interference disappears, and $P_{\bar{e}\bar{e}}$ does not vary with L or E_ν, see eq. (3.2). As a result, the comparison of signals in near and far detectors at reactors will not reveal oscillations. The model predicts a $\bar{\nu}_e$ flux reduction already at the near detector with respect to the initial flux emitted from the reactor. However, establishing this reduction would rely on the ability to determine the original flux with better than 1% accuracy. This seems difficult to achieve.

In contrast to the reactors, in the future long-baseline accelerator experiments T2K [61] and NOνA [62] the damping effect will be quite small, $(1 - e^{-\gamma L}) \simeq \gamma L \sim 0.02$, due to smallness of γ in the GeV energy range. Consequently, the sensitivity of these experiments to $|U_{e3}|^2$ through measurements of $P_{\mu e}$ will be basically unaffected by decoherence. The sensitivity of T2K and NOνA is in the range $\sin^2 2\theta_{13} \gtrsim 0.01$, and therefore these experiments can probe the best fit point of our scenario, eq. (3.3), and large part of the allowed range eq. (3.4), though the lower end of the 3σ interval for $|U_{e3}|^2$ may escape detection. Hence, by comparing the results of T2K and the upcoming reactor experiments, the validity of the present scenario can be tested. The following three situations are of particular interest.

- Comparing the flux at far and near detectors, the reactor experiments such as Double-Chooz and Daya Bay would establish a non-zero value of $|U_{e3}|^2$ in agreement with the value extracted from T2K and NOνA measurements of $P_{\mu e}$. In this case, our scenario would be ruled out because, as discussed above, $P_{\bar{e}\bar{e}}$ at the near and far detectors should be the same.

- Neither the reactor experiments nor the long baseline experiments find any evidence for nonzero $|U_{e3}|^2$ and put an upper bound of 0.0025 on its value ($\sin^2 2\theta_{13} < 0.01$). In this case, the constraints on our scenario become quite tight, and the allowed region for $|U_{e3}|^2$ shifts to the lower end of the 3σ interval given in eq. (3.4). This shifts μ^2 to larger values, of order $1\,\mathrm{eV}^2$ (see figure 2) and increases the tension between LSND and KARMEN data. In order to fully rule out the model, the 3σ bound on $|U_{e3}|^2$ has to be pushed below 0.0014 ($\sin^2 2\theta_{13} < 0.0056$), which probably requires to go beyond the initial phases of T2K and NOνA.

- While comparing the reactor neutrino fluxes at near and far detectors reveals no evidence for missing $\bar{\nu}_e$, T2K and/or NOνA consistently report a value of $|U_{e3}|^2$ in the range $(0.0014, 0.034)$. This situation cannot happen within the standard oscillation scenario. Thus, such an outcome can be considered as a strong hint in favor of our scenario. A way to confirm or refute this hint is to compare the measured reactor neutrino flux with the original flux estimated from the power considerations, as it had been done in the analysis of the CHOOZ data. Of course, to do this the systematical uncertainties in the flux estimations have to be overcome.

JHEP07(2008)067

Currently the MiniBooNE experiment is taking data in the anti-neutrino mode. Since our model invokes neither CP nor CPT violation, the prediction for anti-neutrinos is the same as for neutrinos. Hence one expects a null-result for MiniBooNE anti-neutrino run. For the low energy experiment proposed in ref. [63] using the LENS detector, the situation is similar to the one in the Gallium calibration experiments mentioned above. After very short distances decoherence sets in, leading to a constant event suppression according to eq. (3.2). No distance dependent effect would be observed, and the measurement has to rely on the comparison of expected and predicted numbers of events, which might be difficult due to the normalization uncertainties.

The phase I of T2K is planned to be followed by a phase II which can probe the effects of Δm^2_{21} and, for relatively large values of $|U_{e3}|$ as predicted in our model, measure the Dirac CP-violating phase [61]. The energy of the neutrino flux in the second phase of T2K will be around 750 MeV for which $\gamma \sim \Delta m^2_{21}/E_\nu$. Thus, the decoherence parameter is $(1 - e^{-\gamma L}) \simeq \gamma L \sim \Delta m^2_{21}/\Delta m^2_{31} \simeq 0.03$. Hence, one expects a distortion of the energy spectrum at the level of a few percent. The effect might be difficult to observe in the appearance signal, since in this case, the number of events expected in T2K-II is of order of 1000, i.e., the statistical error is a few percent. Moreover, from eqs. (2.9), we observe that the decoherence effects on the appearance probability, $P_{\mu e}$, is further suppressed with a factor of $|U_{e3}|^2$. However, a spectral distortion due to decoherence is also expected for the ν_μ disappearance signal, where statistics is much larger.

Future projects for superbeam (SPL) or Beta Beam experiments from CERN to a megaton scale detector in Frejus [64] have very good sensitivity to probe our scenario. These experiments will have neutrino energies roughly a factor two smaller than T2K, which enhances γ by a factor 2^r and therefore, $\gamma L \sim \mathcal{O}(1)$. Thus, the experiments would operate in the regime that the decoherence effect is significant and this would lead to very different spectral signatures as compared to standard oscillations.

Ref. [65] suggests to use so-called Mössbauer neutrinos to measure θ_{13}. The energy of such neutrinos is low (for example, for neutrinos from Tritium decay, $E_\nu = 18.60$ keV). For such neutrinos, our scenario predicts eq. (3.2), while within the standard oscillation scenario, $P_{ee} = 1 - 4|U_{e3}|^2(1 - |U_{e3}|^2)\sin^2 \Delta_{31} L/2$ [66]. Considering that the energy spectrum of the Mössbauer neutrinos is monochromatic, it will not be possible to discriminate between the two scenarios by studying the energy dependence of P_{ee}. However, by measuring the flux at several distances it will be possible to make a distinction. If the soft decoherence is realized in nature and the measurement is done at a distance L with $\sin^2 \Delta_{31} L/2 \neq 1/2$, neglecting the decoherence effects will cause a disagreement between the results of T2K and NOνA with this measurement.

4.2 Decoherence in matter; Supernova neutrinos

In matter, the total Hamiltonian includes the interaction term described by the matrix of potentials V: $H \to H + V$. In the neutrino mass basis V is non-diagonal, and therefore $[H, D_n] \neq 0$. The fact that the decoherence matrix does not commute with V and consequently with the total Hamiltonian leads to a new effect: *statistical equilibration* of flavors and masses. This means that after sufficient time ($t \gtrsim ([V, D])^{-1/2}$), ρ converges

to unit matrix times a normalization factor and consequently, in the case of two neutrino mixing, the probabilities of finding neutrinos with the mass m_1 and m_2 in the course of evolution converge to $P_1 = P_2 = 1/2$. Similarly for mixed flavors as a result of long enough evolution $P_e = P_x = 1/2$, where x is some combination of ν_μ and ν_τ neutrinos with which ν_e mixes. This phenomenon is similar to the flavor equilibration in the presence of mixing and inelastic collisions which destroys coherence. Such a type of equilibration has been considered for the active-sterile neutrino oscillations in the Early Universe.

In our scenario non-trivial interplay of the decoherence and matter effect should take place for solar, atmospheric and supernova neutrinos. No significant effect is expected for the solar neutrinos inside the Sun as well the Earth and also for the atmospheric neutrinos inside the Earth. Indeed, for solar neutrinos due to low energies the matter effect on 1-3 mixing is negligible. For atmospheric neutrinos inside the earth the matter effect on 1-3 mixing is substantial in the multi GeV range where decoherence is negligible. In contrast, for supernova neutrinos ($E = 5 - 40\,\mathrm{MeV}$, and huge densities) both matter and decoherence effects are strong.

Let us estimate qualitatively the decoherence effect on supernova neutrinos. In our scenario the 1-3 mixing should be relatively large so that without decoherence the conversion in the H-resonance region (due to 1-3 mixing and mass splitting) should be highly adiabatic. In the case of normal mass hierarchy that would lead to the transition $\nu_e \to \nu_3$ inside the star. As a consequence, no earth matter effect is expected in the neutrino channel. In contrast, in the presence of decoherence and equilibration of mass states only half of ν_e's will end up as ν_3 and another half will transform in the H-resonance region to ν_{2m} - the second eigenstate in matter. Soft decoherence leads to features in supernova neutrinos similar to the ones expected within standard oscillations with $\sin^2 2\theta_{13} < 10^{-4}$; i.e., non-adiabatic conversion in the H-resonance [67]. In particular, the earth matter effect should show up. Thus, one expects mismatch of the 1-3 mixing measured at the accelerators and bound from studies of supernova neutrinos.

Detailed analysis of the decoherence in matter and effects on supernova neutrinos are beyond the scope of this paper. Here we will present a simplified consideration which shows that the statistical equilibration is achieved already before the 1-3 resonance. Recall that in matter the mass states are not the eigenstates of propagation and therefore oscillate. In particular, ν_3 should oscillate into a certain combination of ν_1 and ν_2, ν_a, which depends on the density. In our soft decoherence scenario, the decoherence length for supernova neutrinos ($E \sim (10 - 20)\,\mathrm{MeV}$) is rather small: $L_{\mathrm{decoh}} = 1/\gamma \sim 1$ m. The oscillation length in matter is determined by the refraction length: $l_m \approx 2\pi/V$. Therefore for not very large V we have $L_{\mathrm{decoh}} \ll l_m$. In this limit, the oscillation effect can be considered in the following way. The neutrino trajectory can be divided into intervals of size L_{decoh}. A given mass state, ν_3 oscillates on the first interval L_{decoh} $\nu_3 \to \sqrt{1 - \alpha_1^2}\nu_3 + \alpha_1\nu_a$, where $|\alpha_1|^2 = P_1$ is the transition probability. At the end of this interval the coherence between ν_3 and ν_a components of the state is destroyed and in the next interval, L_{decoh}, they will oscillate independently. At the end of the second interval we will have split of the states again, and so forth. The probability of transition $\nu_3 \to \nu_a$ in the ith interval, $P_i \ll 1$ can

JHEP07(2008)067

be estimated as

$$P_i \sim \sin^2 2\theta^m_{\rm mass}(V_i)\, \sin^2\phi_i \approx \sin^2 2\theta^m_{\rm mass}(V_i)\, \phi_i^2 \approx \sin^2 2\theta_{13}\, (V_i L_{\rm decoh})^2\,, \qquad (4.1)$$

where $\theta^m_{\rm mass} = \theta^m_{13} - \theta_{13}$ is the mixing angle of the mass states in matter (θ^m_{13} is the mixing angle of the flavor states in matter), V_i is the matter potential in the ith interval, ϕ_i is the half-phase of oscillations in the ith interval . Notice that to derive eq. (23) we have used the constant density approximation for the oscillation probability within each interval of size $L_{\rm decoh}$. We have then used $\phi_i \ll 1$ which follows from $L_{\rm decoh} \ll l_m$.

Since the initial flux is mainly composed of ν_3, the flux transition $\nu_3 \to \nu_a$ will dominate over the opposite transition $\nu_a \to \nu_3$, and eventually this will lead to the equilibration of the ν_3 and ν_a fluxes. The total transition probability after passing n intervals is given by

$$P \approx \sum_i^n P_i = \sum_i^n \sin^2 2\theta_{13} V_i^2 L^2_{\rm decoh}\,. \qquad (4.2)$$

This formula is valid when $P \ll 1$ (linear regime) for which the inverse transition still can be neglected. Still the condition $P \sim 1$ allows to evaluate the length (numbers of intervals) over which the equilibration is achieved. Substituting summation in (4.2) by integration we obtain

$$P \approx \sin^2 2\theta_{13} L_{\rm decoh} \int_{r_0}^{r_R} V^2(r) dr\,, \qquad (4.3)$$

where $r_R \sim 10^7$ m is the radius of the resonance layer. (Recall we are estimating the distance from the resonance layer in the direction of center of a star on which equilibration is reached.) Taking $V = V_R(r_R/r)^3$ we obtain from (4.3)

$$P \approx \sin^2 2\theta_{13} [L_{\rm decoh} V(r_0)]^2 \frac{r_0}{5 L_{\rm decoh}}\,. \qquad (4.4)$$

Taking $V_R \sim \Delta m^2_{13}/E_\nu$, from eq. (4.3), we find that for the whole range of θ_{13} within our scenario [see eq. (3.4)], propagating from $r_0 \sim 0.1 r_R$ to r_R the equilibration condition ($P \sim 1$) is fulfilled.

5. Conclusions

Clearly there is no simple explanation of the LSND result which is consistent with other neutrino data. According to some proposals it requires the combination of two exotic mechanisms. One can ask if any yet unknown mechanism exists which can provide a description of (reconcile) all the data. One can take the bottom up approach and try to uncover properties (energy and distance dependence) of this unknown mechanism. Our proposal is essentially along this line.

We have proposed an explanation of the LSND signal as manifestation of the quantum decoherence of mass states associated to the 1-3 mixing and mass splitting. The decoherence leads to a complete or partial damping of the interference terms in the oscillation probabilities. Our phenomenological scenario is based on the three-neutrino framework (without any sterile neutrinos) and makes use of a single decoherence parameter γ with

JHEP07(2008)067

a sharp energy dependence (soft decoherence). The main features of our scenario, which allow us to reconcile the LSND signal with the results of other experiments are:

- zero or negligible decoherence effect on the 1-2 mixing and splitting ($\gamma_{12} = 0$);
- decoherence of only the ν_3 mass eigenstate;
- a strong decrease of the decoherence effect with the neutrino energy: $\gamma \equiv \gamma_{13} = \gamma_{23} \propto E_\nu^{-r}$.

The strong decrease of γ with energy allows us to accommodate the LSND signal, while being consistent with the null-results of experiments at higher energies, such as MiniBooNE, CDHS, NOMAD, and NuTeV. At the same time this energy dependence guarantees standard neutrino oscillations in the atmospheric and MINOS experiments. The lower bound on the energy exponent, $r \gtrsim 4$, follows from the low energy atmospheric neutrino data; $r = 4$ can be considered as an optimal reference value. The assumption $\gamma_{12} = 0$ ensures that oscillations in the 1-2 sector relevant for solar neutrinos and the KamLAND experiment are not affected.

Within the present scenario the KARMEN-LSND tension still persists. As shown in table 1, the probability of consistency of LSND with null-result experiments is 1.4%. In the case of soft-decoherence this somewhat low value is a consequence of the constraint from KARMEN. In constrast, for (3+2) sterile neutrino oscillations this probability is only 0.08% due to the additional tension between appearance and disappearance experiments, which is fully resolved for soft-decoherence.

The LSND signal is determined by the mixing angle θ_{13}, and the degree of decoherence. It implies a lower bound on 1-3 mixing, $\sin^2 2\theta_{13} > 0.006$ (3σ), which corresponds to complete decoherence. This in turn, leads to testable predictions for upcoming experimental searches of 1-3 mixing. For reactor experiments (MeV energies) like Double-Chooz or Daya Bay we predict full decoherence already after a few centimeters, leading to no oscillation effect when results from near and far detectors are compared. In contrast, the long-baseline accelerator experiments (GeV energy range) like T2K or NOνA are practically not affected by decoherence and a signal for θ_{13} should show up. Hence, a mismatch in the θ_{13} measurements of upcoming reactor and accelerator long baseline experiments would be a clear indication for the proposed scenario. At low-energy long-baseline experiments such as the CERN SPL superbeam or a Beta Beam with a relativistic γ-factor of 100, our decoherence scenario will lead to a distinct energy spectrum of the appearance as well as disappearance signals. The soft decoherence can also show up as a distortion in the energy dependence of disappearance probability in the second phase T2K. This scenario can also partially account for the anomaly found in Gallium radioactive source experiments [55], though explaining the full effect might be difficult. Soft decoherence can also affect the supernova neutrinos. Despite relatively large θ_{13}, decoherence leads to a neutrino composition similar to the case of non-adiabatic conversion which takes place in the case of the standard oscillation with $\sin^2 2\theta_{13} < 10^{-4}$. Thus, comparing θ_{13} measured by T2K and NOνA and supernova bound on this mixing angle can be considered as another way to test the present scenario.

JHEP07(2008)067

The energy dependence of the decoherence effect has to be explained by an underlying theory that gives rise to quantum decoherence. In this paper we considered the simplest power law dependence of γ in the whole energy range. In general γ may have a more complicated dependence. Indeed, the fact that $\gamma \to \infty$ for $E_\nu \to 0$ indicates that there should be some low energy cut-off below which the dependence of γ on E_ν becomes modified. The restrictions on γ come from neutrino data in the energy range from $\sim 10\,\mathrm{MeV}$ to multi-GeV. With a general energy dependence, it is possible that for $E_\nu < 10\,\mathrm{MeV}$, γ remains constant or even becomes small again. Such a behavior could modify our predictions for low energy experiments, especially reactor neutrinos. Note, however, that under the power law assumption the coherence for reactor neutrinos is lost already within a few cm, whereas the close detectors are at several hundred meters. So, if γ is constant below LSND energies or even decreases not very fast, we still will have decoherence. Hence, most probably at least partial decoherence will be observed and in this case still 1-3 mixing will be different in reactor and accelerator experiments. Only in the case of a very sharp cut-off below $E_\nu \sim 10\,\mathrm{MeV}$ (a behavior which appears quite unnatural) one will see the same 1-3 mixings in both cases. In any case the decoherence can be still probed by studies of the energy spectrum in the phase II of T2K, and CERN beta beam and SPL experiments. Moreover, we still expect a disagreement between θ_{13} measurements by T2K and NOνA and the bounds from supernova data.

Finally, we point out that in the minimal scenario presented in this paper, the event excess at low energies ($E_\nu < 475\,\mathrm{MeV}$) found in MiniBooNE [14] cannot be explained. From eq. (2.9), we observe that in the range $\gamma L \sim 1$, a small value of $P_{\mu e}$ explaining the anomaly observed by MiniBooNE implies a significant deviation of $P_{\mu\mu}$, $\mathcal{O}(P_{e\mu}/|U_{e3}|^2)$, from the standard neutrino oscillation scenario. Lack of any evidence for such deviation in low energy ($E_\nu < 475\,\mathrm{MeV}$) atmospheric neutrino data rules out this explanation. In order to accommodate the low energy MiniBooNE data consistently with the low energy atmospheric neutrino data, in addition to the decoherence matrix that explains the LSND data, one should introduce another decoherence matrix D' that violates energy conservation. With a special flavor structure for D', it is then possible to suppress the deviation of $P_{\mu\mu}$ from the standard oscillation prediction. In order to avoid the bounds from NuTeV [13], D' has to vanish for higher energies. Of course, after adding the new decoherence matrix, D', the scenario loses the simple features of the minimal coherence scenario discussed in this paper.

Acknowledgments

We thank Michele Maltoni and W. Louis for useful communications. A. Yu. S. acknowledges some early discussions of the decoherence and LSND result with Srubabati Goswami. Y. F. thanks ICTP where part of this work has been done for its support and the hospitality of its staff. She is also grateful to Ashoke Sen for useful discussions. T. S. would like to thank Alexander Sakharov for discussions on decoherence due to quantum gravity.

JHEP07(2008)067

References

[1] LSND collaboration, A. Aguilar et al., *Evidence for neutrino oscillations from the observation of $\bar{\nu}/e$ appearance in a anti-ν_μ beam*, *Phys. Rev.* **D 64** (2001) 112007 [hep-ex/0104049].

[2] Super-Kamiokande collaboration, Y. Ashie et al., *A measurement of atmospheric neutrino oscillation parameters by Super-Kamiokande I*, *Phys. Rev.* **D 71** (2005) 112005 [hep-ex/0501064].

[3] MINOS collaboration, D.G. Michael et al., *Observation of muon neutrino disappearance with the MINOS detectors and the NuMI neutrino beam*, *Phys. Rev. Lett.* **97** (2006) 191801 [hep-ex/0607088].

[4] K2K collaboration, M.H. Ahn et al., *Measurement of neutrino oscillation by the K2K experiment*, *Phys. Rev.* **D 74** (2006) 072003 [hep-ex/0606032].

[5] SNO collaboration, Q.R. Ahmad et al., *Direct evidence for neutrino flavor transformation from neutral-current interactions in the Sudbury Neutrino Observatory*, *Phys. Rev. Lett.* **89** (2002) 011301 [nucl-ex/0204008].

[6] KamLAND collaboration, T. Araki et al., *Measurement of neutrino oscillation with KamLAND: evidence of spectral distortion*, *Phys. Rev. Lett.* **94** (2005) 081801 [hep-ex/0406035].

[7] CHOOZ collaboration, M. Apollonio et al., *Search for neutrino oscillations on a long base-line at the CHOOZ nuclear power station*, *Eur. Phys. J.* **C 27** (2003) 331 [hep-ex/0301017].

[8] F. Boehm et al., *Final results from the Palo Verde neutrino oscillation experiment*, *Phys. Rev.* **D 64** (2001) 112001 [hep-ex/0107009].

[9] KARMEN collaboration, B. Armbruster et al., *Upper limits for neutrino oscillations $\bar{\nu}_\mu \to \bar{\nu}/e$ from muon decay at rest*, *Phys. Rev.* **D 65** (2002) 112001 [hep-ex/0203021].

[10] F. Dydak et al., *A search for muon-neutrino oscillations in the ΔM^2 range* 0.3 eVq *to* 90 eVq, *Phys. Lett.* **B 134** (1984) 281.

[11] Y. Declais et al., *Search for neutrino oscillations at* 15*-meters,* 40*-meters, and* 95*-meters from a nuclear power reactor at Bugey*, *Nucl. Phys.* **B 434** (1995) 503.

[12] NOMAD collaboration, P. Astier et al., *Search for $\nu_\mu \to \nu_e$ oscillations in the NOMAD experiment*, *Phys. Lett.* **B 570** (2003) 19 [hep-ex/0306037].

[13] S. Avvakumov et al., *A search for $\nu_\mu \to \nu_e$ and $\bar{\nu}_\mu \to \bar{\nu}/e$ oscillations at NuTeV*, *Phys. Rev. Lett.* **89** (2002) 011804 [hep-ex/0203018].

[14] The MiniBooNE collaboration, A.A. Aguilar-Arevalo et al., *A search for electron neutrino appearance at the $\Delta m^2 \sim 1eV^2$ scale*, *Phys. Rev. Lett.* **98** (2007) 231801 [arXiv:0704.1500].

[15] MiniBooNE collaboration and others, *Compatibility of high-Δm^2 ν_e and $\bar{\nu}_e$ neutrino oscillation searches*, arXiv:0805.1764.

[16] M. Maltoni, T. Schwetz, M.A. Tortola and J.W.F. Valle, *Ruling out four-neutrino oscillation interpretations of the LSND anomaly?*, *Nucl. Phys.* **B 643** (2002) 321 [hep-ph/0207157].

[17] M. Maltoni and T. Schwetz, *Sterile neutrino oscillations after first MiniBooNE results*, *Phys. Rev.* **D 76** (2007) 093005 [arXiv:0705.0107].

JHEP07(2008)067

[18] E. Ma, G. Rajasekaran and I. Stancu, *Hierarchical four-neutrino oscillations with a decay option*, *Phys. Rev.* **D 61** (2000) 071302 [hep-ph/9908489];
E. Ma and G. Rajasekaran, *Light unstable sterile neutrino*, *Phys. Rev.* **D 64** (2001) 117303 [hep-ph/0107203].

[19] S. Palomares-Ruiz, S. Pascoli and T. Schwetz, *Explaining LSND by a decaying sterile neutrino*, *JHEP* **09** (2005) 048 [hep-ph/0505216].

[20] H. Murayama and T. Yanagida, *LSND, SN1987A and CPT violation*, *Phys. Lett.* **B 520** (2001) 263 [hep-ph/0010178];
G. Barenboim, L. Borissov, J.D. Lykken and A.Y. Smirnov, *Neutrinos as the messengers of CPT violation*, *JHEP* **10** (2002) 001 [hep-ph/0108199];
G. Barenboim, L. Borissov and J.D. Lykken, *CPT violating neutrinos in the light of KamLAND*, hep-ph/0212116;
M.C. Gonzalez-Garcia, M. Maltoni and T. Schwetz, *Status of the CPT violating interpretations of the LSND signal*, *Phys. Rev.* **D 68** (2003) 053007 [hep-ph/0306226];
V. Barger, D. Marfatia and K. Whisnant, *LSND anomaly from CPT violation in four-neutrino models*, *Phys. Lett.* **B 576** (2003) 303 [hep-ph/0308299].

[21] V.A. Kostelecky and M. Mewes, *Lorentz violation and short-baseline neutrino experiments*, *Phys. Rev.* **D 70** (2004) 076002 [hep-ph/0406255];
A. de Gouvêa and Y. Grossman, *A three-flavor, Lorentz-violating solution to the LSND anomaly*, *Phys. Rev.* **D 74** (2006) 093008 [hep-ph/0602237];
T. Katori, V.A. Kostelecky and R. Tayloe, *Global three-parameter model for neutrino oscillations using Lorentz violation*, *Phys. Rev.* **D 74** (2006) 105009 [hep-ph/0606154].

[22] D.B. Kaplan, A.E. Nelson and N. Weiner, *Neutrino oscillations as a probe of dark energy*, *Phys. Rev. Lett.* **93** (2004) 091801 [hep-ph/0401099];
K.M. Zurek, *New matter effects in neutrino oscillation experiments*, *JHEP* **10** (2004) 058 [hep-ph/0405141];
V. Barger, D. Marfatia and K. Whisnant, *Confronting mass-varying neutrinos with MiniBooNE*, *Phys. Rev.* **D 73** (2006) 013005 [hep-ph/0509163].

[23] H. Pas, S. Pakvasa and T.J. Weiler, *Sterile-active neutrino oscillations and shortcuts in the extra dimension*, *Phys. Rev.* **D 72** (2005) 095017 [hep-ph/0504096].

[24] T. Schwetz, *LSND versus MiniBooNE: sterile neutrinos with energy dependent masses and mixing?*, *JHEP* **02** (2008) 011 [arXiv:0710.2985].

[25] A.E. Nelson and J. Walsh, *Short baseline neutrino oscillations and a new light gauge boson*, *Phys. Rev.* **D 77** (2008) 033001 [arXiv:0711.1363].

[26] G. Barenboim and N.E. Mavromatos, *CPT violating decoherence and LSND: a possible window to Planck scale physics*, *JHEP* **01** (2005) 034 [hep-ph/0404014].

[27] G. Barenboim, N.E. Mavromatos, S. Sarkar and A. Waldron-Lauda, *Quantum decoherence and neutrino data*, *Nucl. Phys.* **B 758** (2006) 90 [hep-ph/0603028].

[28] S.W. Hawking, *Particle creation by black holes*, *Commun. Math. Phys.* **43** (1975) 199;
Breakdown of predictability in gravitational collapse, *Phys. Rev.* **D 14** (1976) 2460.

[29] J.R. Ellis, J.S. Hagelin, D.V. Nanopoulos and M. Srednicki, *Search for violations of quantum mechanics*, *Nucl. Phys.* **B 241** (1984) 381.

[30] S.B. Giddings and A. Strominger, *Loss of incoherence and determination of coupling constants in quantum gravity*, *Nucl. Phys.* **B 307** (1988) 854.

JHEP07(2008)067

[31] N.E. Mavromatos and S. Sarkar, *Probing models of quantum decoherence in particle physics and cosmology*, hep-ph/0612193.

[32] E. Lisi, A. Marrone and D. Montanino, *Probing possible decoherence effects in atmospheric neutrino oscillations*, *Phys. Rev. Lett.* **85** (2000) 1166 [hep-ph/0002053];
G.L. Fogli, E. Lisi, A. Marrone and D. Montanino, *Status of atmospheric $\nu_\mu \to \nu_\tau$ oscillations and decoherence after the first K2K spectral data*, *Phys. Rev.* **D 67** (2003) 093006 [hep-ph/0303064].

[33] G.L. Fogli, E. Lisi, A. Marrone, D. Montanino and A. Palazzo, *Probing non-standard decoherence effects with solar and KamLAND neutrinos*, *Phys. Rev.* **D 76** (2007) 033006 [arXiv:0704.2568].

[34] T. Schwetz, *Variations on KamLAND: likelihood analysis and frequentist confidence regions*, *Phys. Lett.* **B 577** (2003) 120 [hep-ph/0308003].

[35] M. Blennow, T. Ohlsson and W. Winter, *Damping signatures in future neutrino oscillation experiments*, *JHEP* **06** (2005) 049 [hep-ph/0502147].

[36] N.E. Mavromatos, A. Meregaglia, A. Rubbia, A. Sakharov and S. Sarkar, *Quantum-gravity decoherence effects in neutrino oscillations: expected constraints from CNGS and J-PARC*, *Phys. Rev.* **D 77** (2008) 053014 [arXiv:0801.0872].

[37] D.V. Ahluwalia, *Ambiguity in source flux of cosmic/astrophysical neutrinos: effects of bi-maximal mixing and quantum-gravity induced decoherence*, *Mod. Phys. Lett.* **A 16** (2001) 917 [hep-ph/0104316];
D. Hooper, D. Morgan and E. Winstanley, *Probing quantum decoherence with high-energy neutrinos*, *Phys. Lett.* **B 609** (2005) 206 [hep-ph/0410094];
L.A. Anchordoqui et al., *Probing Planck scale physics with IceCube*, *Phys. Rev.* **D 72** (2005) 065019 [hep-ph/0506168];
Y. Farzan and A.Y. Smirnov, *Coherence and oscillations of cosmic neutrinos*, arXiv:0803.0495.

[38] C.P. Sun and D.L. Zhou, *Quantum decoherence effect and neutrino oscillation*, hep-ph/9808334;
A.M. Gago, E.M. Santos, W.J.C. Teves and R. Zukanovich Funchal, *A study on quantum decoherence phenomena with three generations of neutrinos*, hep-ph/0208166.

[39] P. Huet and M.E. Peskin, *Violation of CPT and quantum mechanics in the K_0-$\bar{K}_0$ system*, *Nucl. Phys.* **B 434** (1995) 3 [hep-ph/9403257];
J.R. Ellis, J.L. Lopez, N.E. Mavromatos and D.V. Nanopoulos, *Precision tests of CPT symmetry and quantum mechanics in the neutral kaon system*, *Phys. Rev.* **D 53** (1996) 3846 [hep-ph/9505340];
F. Benatti and R. Floreanini, *Complete positivity and the $K\bar{K}$ system*, *Phys. Lett.* **B 389** (1996) 100 [hep-th/9607059];
R.A. Bertlmann, W. Grimus and B.C. Hiesmayr, *Quantum mechanics, Furry's hypothesis and a measure of decoherence in the K_0 $\bar{K}_0$ system*, *Phys. Rev.* **D 60** (1999) 114032 [hep-ph/9902427].

[40] CPLEAR collaboration, R. Adler et al., *Test of CPT symmetry and quantum mechanics with experimental data from CPLEAR*, *Phys. Lett.* **B 364** (1995) 239 [hep-ex/9511001];
KLOE collaboration, F. Ambrosino et al., *First observation of quantum interference in the process $\Phi \to K(S)K(L) \to \pi^+\pi^-\pi^+\pi^-$: a test of quantum mechanics and CPT symmetry*, *Phys. Lett.* **B 642** (2006) 315 [hep-ex/0607027].

JHEP07(2008)067

[41] R.A. Bertlmann and W. Grimus, *How devious are deviations from quantum mechanics: the case of the B^0-$\bar{B}^0$ system*, *Phys. Rev.* **D 58** (1998) 034014 [hep-ph/9710236]; *A model for decoherence of entangled beauty*, *Phys. Rev.* **D 64** (2001) 056004 [hep-ph/0101160].

[42] Belle collaboration, A. Go et al., *Measurement of EPR-type flavour entanglement in $\Upsilon(4S) \to B^0$-$\bar{B}^0$ decays*, *Phys. Rev. Lett.* **99** (2007) 131802 [quant-ph/0702267].

[43] F. Benatti and R. Floreanini, *Complete positivity and neutron interferometry*, *Phys. Lett.* **B 451** (1999) 422 [quant-ph/9902026].

[44] G. Lindblad, *On the generators of quantum dynamical semigroups*, *Commun. Math. Phys.* **48** (1976) 119.

[45] T. Banks, L. Susskind and M.E. Peskin, *Difficulties for the evolution of pure states into mixed states*, *Nucl. Phys.* **B 244** (1984) 125.

[46] S.L. Adler, *Derivation of the Lindblad generator structure by use of the Itô stochastic* , *Phys. Lett.* **A 265** (2000) 58 [*Corrigendum ibid.* **267** (2000) 212].

[47] F. Benatti and H. Narnhofer, *Entropy behavior under completely positive maps*, *Lett. Math. Phys.* **15** (1988) 325.

[48] Technical data on the MiniBooNE oscillation analysis is available at the webpage http://www-boone.fnal.gov/for_physicists/april07datarelease/.

[49] W. Grimus and T. Schwetz, *4-neutrino mass schemes and the likelihood of $(3+1)$-mass spectra*, *Eur. Phys. J.* **C 20** (2001) 1 [hep-ph/0102252].

[50] E.D. Church, K. Eitel, G.B. Mills and M. Steidl, *Statistical analysis of different $\bar{\nu}_\mu \to \bar{\nu}_e$ searches*, *Phys. Rev.* **D 66** (2002) 013001 [hep-ex/0203023].

[51] M. Sorel, J.M. Conrad and M. Shaevitz, *A combined analysis of short-baseline neutrino experiments in the $(3+1)$ and $(3+2)$ sterile neutrino oscillation hypotheses*, *Phys. Rev.* **D 70** (2004) 073004 [hep-ph/0305255].

[52] M. Maltoni and T. Schwetz, *Testing the statistical comPatibility of independent data sets*, *Phys. Rev.* **D 68** (2003) 033020 [hep-ph/0304176].

[53] G. Karagiorgi et al., *Leptonic CP-violation studies at MiniBooNE in the $(3+2)$ sterile neutrino oscillation hypothesis*, *Phys. Rev.* **D 75** (2007) 013011 [hep-ph/0609177];
J.T. Goldman, J. Stephenson, G. J. and B.H.J. McKellar, *Multichannel oscillations and relations between LSND, KARMEN and MiniBooNE, with and without CP-violation*, *Phys. Rev.* **D 75** (2007) 091301 [nucl-th/0703023].

[54] Soudan 2 collaboration, M.C. Sanchez et al., *Observation of atmospheric neutrino oscillations in Soudan 2*, *Phys. Rev.* **D 68** (2003) 113004 [hep-ex/0307069].

[55] D.N. Abdurashitov et al., *The Russian-American gallium experiment (SAGE) Cr neutrino source measurement*, *Phys. Rev. Lett.* **77** (1996) 4708;
SAGE collaboration, J.N. Abdurashitov et al., *Measurement of the response of the Russian-American gallium experiment to neutrinos from a Cr-51 source*, *Phys. Rev.* **C 59** (1999) 2246 [hep-ph/9803418];
J.N. Abdurashitov et al., *Measurement of the response of a Ga solar neutrino experiment to neutrinos from an Ar-37 source*, *Phys. Rev.* **C 73** (2006) 045805 [nucl-ex/0512041].

JHEP07(2008)067

[56] GALLEX. collaboration, P. Anselmann et al., *First results from the Cr-51 neutrino source experiment with the GALLEX detector*, *Phys. Lett.* **B 342** (1995) 440;
GALLEX collaboration, W. Hampel et al., *Final results of the Cr-51 neutrino source experiments in GALLEX*, *Phys. Lett.* **B 420** (1998) 114.

[57] C. Giunti and M. Laveder, *Short-baseline active-sterile neutrino oscillations?*, *Mod. Phys. Lett.* **A 22** (2007) 2499 [hep-ph/0610352];
M.A. Acero, C. Giunti and M. Laveder, *Limits on ν_e and $\bar{\nu}_e$ disappearance from Gallium and reactor experiments*, arXiv:0711.4222.

[58] Double CHOOZ collaboration, F. Ardellier et al., *Double CHOOZ: a search for the neutrino mixing angle θ_{13}*, hep-ex/0606025.

[59] Daya Bay collaboration, X. Guo et al., *A precision measurement of the neutrino mixing angle θ_{13} using reactor antineutrinos at Daya Bay*, hep-ex/0701029.

[60] See http://neutrino.snu.ac.kr/RENO/INTRO/intro.html.

[61] The T2K collaboration, Y. Itow et al., *The JHF-Kamioka neutrino project*, hep-ex/0106019.

[62] NOvA collaboration, D.S. Ayres et al., *NOvA proposal to build a 30-kiloton off-axis detector to study neutrino oscillations in the Fermilab NuMI beamline*, hep-ex/0503053.

[63] C. Grieb, J. Link and R.S. Raghavan, *Probing active to sterile neutrino oscillations in the LENS detector*, *Phys. Rev.* **D 75** (2007) 093006 [hep-ph/0611178].

[64] J.E. Campagne, M. Maltoni, M. Mezzetto and T. Schwetz, *Physics potential of the CERN-MEMPHYS neutrino oscillation project*, *JHEP* **04** (2007) 003 [hep-ph/0603172].

[65] R.S. Raghavan, *Recoilless resonant capture of antineutrinos*, hep-ph/0511191.

[66] E.K. Akhmedov, J. Kopp and M. Lindner, *Oscillations of Mössbauer neutrinos*, *JHEP* **05** (2008) 005 [arXiv:0802.2513]; *On application of the time-energy uncertainty relation to Mössbauer neutrino experiments*, arXiv:0803.1424;
see however, S.M. Bilenky, F. von Feilitzsch and W. Potzel, *Time-energy uncertainty relations for neutrino oscillation and Mössbauer neutrino experiment*, arXiv:0803.0527; *Different schemes of neutrino oscillations in Mössbauer neutrino experiment*, arXiv:0804.3409.

[67] A.S. Dighe and A.Y. Smirnov, *Identifying the neutrino mass spectrum from the neutrino burst from a supernova*, *Phys. Rev.* **D 62** (2000) 033007 [hep-ph/9907423].

JHEP07(2008)067